AD-A183 851 A GENERALIZED LEAST-SQUARES DETERMINATION OF TRIAXIAL STRESS STATES BY X- (U) NORTHWESTERN UNIV EVANSTON IL DEPT OF MATERIALS SCIENCE AND E R A WINHOLTZ ET AL 1/1

UNCLASSIFIED JUL 87 TR-25 N00014-80-C-0116 F/G 20/11 NL

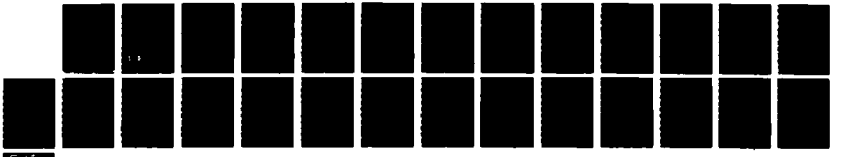

END
7 87
DTIC

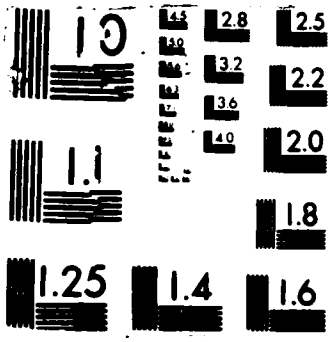
2.8
2.5
3.2
2.2
3.6
2.0
1.8
1.1
1.25
1.4
1.6

(12)

NORTHWESTERN UNIVERSITY

DEPARTMENT OF MATERIALS SCIENCE

TECHNICAL REPORT # 25
JULY 1987

OFFICE OF NAVAL RESEARCH
CONTRACT NO. N00014-80-C-116

A GENERALIZED LEAST-SQUARES DETERMINATION OF TRIAXIAL STRESS STATES BY X-RAY DIFFRACTION AND THE ASSOCIATED ERRORS

BY

R. A. WINHOLTZ AND J. B. COHEN

EVANSTON, ILLINOIS

A GENERALIZED LEAST-SQUARES DETERMINATION OF TRIAXIAL STRESS STATES BY X-RAY DIFFRACTION AND THE ASSOCIATED ERRORS

R.A. Winholtz and J.B. Cohen

Department of Materials Science and Engineering
The Technological Institute
Northwestern University
Evanston, IL 60201, USA

ABSTRACT

The determination of residual stresses via x-ray diffraction is briefly reviewed, with particular emphasis on the triaxial stress state. A new method is proposed for determining the general stress tensor, which considerably reduces the variances of the stresses due to counting statistics and gradients. The procedure involves a generalized least square solution of strains measured at various tilts of the x-ray beam to the sample, and a set of tilts not heretofore used is recommended to minimize these errors.

1. INTRODUCTION

X-ray diffraction can be used to determine stresses by measuring the changes in interplanar spacing in a crystalline material. Classical stress determination using x-ray diffraction assumes a biaxial stress state where the stresses normal to the surface are zero. This assumption leads to equations from which the stress along the measurement direction σ_ϕ may be determined from the slope of a d versus $\sin^2\psi$ plot (Noyan and Cohen 1987). The angles ϕ and ψ are defined in Figure 1 and d is the interplanar spacing perpendicular to the L_3 axis.

Triaxial stress states cause curvature in the d versus $\sin^2\psi$ plots (Noyan and Cohen 1984). This curvature has been observed in several experimental studies (Dölle and Cohen 1980; Ho et al. 1983). The presence of a stress normal to the surface, σ_{33}, will cause curvature in d versus $\sin^2\psi$ plots while the shear

stresses σ_{13} and σ_{23} produce different curves for negative and positive ψ-tilts (ψ-splitting). Dölle and Hauk have extended the classical stress analysis theory to include the determination of triaxial stress states (Dölle and Hauk 1976; Dölle 1979). This method uses the average strain for positive and negative ψ-tilts versus $\sin^2\psi$ at ϕ equal to 0°, 45°, and 90° to determine the stresses σ_{11}, σ_{22}, σ_{33}, and σ_{12}. The stresses σ_{13} and σ_{23} are determined from plots of the difference in strain for positive and negative ψ-tilts versus $\sin 2\psi$.

In this paper a generalized least-squares method of determining triaxial residual stresses from diffraction data is presented. Being able to estimate the errors associated with a measurement is also quite important. Errors due to counting statistics and stress gradients with the Dölle-Hauk method have been investigated by Rudnik and Cohen (1986), Noyan (1983), and Noyan and Cohen (1980). These errors are investigated for the generalized least-squares method and it is shown that the method is less sensitive to errors than the Dölle-Hauk method.

2. THEORY

Consider the two coordinate systems in Figure 1. The P-coordinate system is attached to the sample and is the coordinate system in which it is desired to measure the stresses. The L-coordinate system is the laboratory system and is the system in which the diffraction measurements are made. The two

coordinate systems are oriented with respect to each other by the angles ϕ and ψ. One may determine the interplanar spacing along planes perpendicular to the L_3 axis, $d_{\phi\psi}$, from the position of a diffraction peak. By knowing the unstressed planar spacing d_o one may determine the strain along the L_3 axis.

$$e_{\phi\psi} = \frac{d_{\phi\psi} - d_o}{d_o} \quad . \tag{1}$$

Noyan (1985) discusses several methods of determining d_o. Using tensor transformations the strains in the P-coordinate system may be related to the stain along the L_3 axis as

$$\begin{aligned} e_{\phi\psi} = {} & \varepsilon_{11}\cos^2\phi\sin^2\psi + \varepsilon_{22}\sin^2\phi\sin^2\psi + \varepsilon_{33}\cos^2\psi + \\ & \varepsilon_{12}\sin 2\phi\sin^2\psi + \varepsilon_{13}\cos\phi\sin 2\Psi + \varepsilon_{23}\sin\phi\sin 2\psi. \end{aligned} \tag{2}$$

The ε_{ij} refer to strains in the sample coordinate system while $e_{\phi\psi}$ refers to strains measured in the laboratory coordinate system.

Equation 2 shows that the measured strains, $e_{\phi\psi}$, are linear with respect to the strains in the sample coordinate system. Measuring strains in six independent directions is therefore sufficient to determine the strains ε_{ij} (Nye 1976). The accuracy may be improved by measuring more than six strains $e_{\phi\psi}$ and determining the strains ε_{ij} by a least-squares procedure (Imura et al. 1962).

To facilitate a matrix formulation of the least-squares procedure the following definitions are made:

$$\begin{aligned} \varepsilon_1 &= \varepsilon_{11} & f_1(\phi,\Psi) &= \cos^2\phi\sin^2\Psi \\ \varepsilon_2 &= \varepsilon_{22} & f_2(\phi,\Psi) &= \sin^2\phi\sin^2\Psi \\ \varepsilon_3 &= \varepsilon_{33} & f_3(\phi,\Psi) &= \cos^2\Psi \\ \varepsilon_4 &= \varepsilon_{12} & f_4(\phi,\Psi) &= \sin 2\phi\sin^2\Psi \\ \varepsilon_5 &= \varepsilon_{13} & f_5(\phi,\Psi) &= \cos\phi\sin 2\Psi \\ \varepsilon_6 &= \varepsilon_{23} & f_6(\phi,\Psi) &= \sin\phi\sin 2\Psi \ . \end{aligned}$$

The residual between the measured and calculated strain along the L_3 axis is

$$r_i = \sum_{j=1}^{6} \varepsilon_j f_j(\phi_i,\Psi_i) - e_i \qquad (3)$$

The total weighted sum of the squared error, R, for n measurements of e is then :

$$R = \sum_{i=1}^{n} \frac{1}{\mathrm{var}(e_i)} \left\{ \left[\sum_{j=1}^{6} \varepsilon_j f_j(\phi_i,\Psi_i) \right] - e_i \right\}^2 \ . \qquad (4)$$

Each error r_i is weighted by the inverse variance associated with the corresponding strain e_i. Equations exist for estimating these variances from the diffraction data (James and Cohen 1977) as discussed below. Thus, the most reliable measurements are weighted the most. Taking the partial derivative with respect to each strain ε_j and setting them equal to zero to find the minimum, results in the set of equations;

$$\sum_{i=1}^{n} \left[\left(\sum_{k=1}^{6} \varepsilon_k f_k(\phi_i,U_i) \right) - e_i \right] \frac{f_j(\phi_i,U_i)}{\mathrm{var}(e_i)} = 0 \ . \qquad (5)$$

To formulate a matrix equation the B-matrix and E-vector are defined as

$$B_{jk} = \sum_{i=1}^{n} \frac{f_j(\phi_i,\Psi_i) f_k(\phi_i,\Psi_i)}{\mathrm{var}(e_i)} \ , \qquad (6)$$

$$E_j = \sum_{i=1}^{n} e_i f_j(\phi_i,\Psi_i)/\mathrm{var}(e_i) \ . \qquad (7)$$

Provided that the strains are measured at ϕ and ψ angles that do not form a singular B-matrix, the strains giving the least squared error are given by the solution of the equation:

$$\underline{\underline{B}}\,\underline{\varepsilon} = \underline{E} \,, \tag{8}$$

or

$$\underline{\varepsilon} = \underline{\underline{B}}^{-1}\underline{E} \,. \tag{9}$$

When the strains have been determined the stresses may be determined from the relations:

$$\sigma_{ij} = \frac{1}{S_2/2}[\varepsilon_{ij} - \delta_{ij}\frac{S_1}{S_2/2 + 3S_1}(\varepsilon_{11} + \varepsilon_{22} + \varepsilon_{33})] \tag{10}$$

where S_1 and $S_2/2$ are the appropriate x-ray elastic constants (Marion and Cohen 1977; Perry et al. 1984) and δ_{ij} is the Kronecker delta function. The stresses may also be obtained directly by substituting σ for ε and the functions g_j for the functions f_j in Equations 6, 7, and 8, where:

$$\begin{aligned}
g_1(\phi,\psi) &= (\cos^2\phi\sin^2\psi)S_2/2 - S_1 \\
g_2(\phi,\psi) &= (\sin^2\phi\sin^2\psi)S_2/2 - S_1 \\
g_3(\phi,\psi) &= (\cos^2\psi)S_2/2 - S_1 \\
g_4(\phi,\psi) &= (\sin 2\phi\sin^2\psi)S_2/2 \\
g_5(\phi,\psi) &= (\cos\phi\sin 2\psi)S_2/2 \\
g_6(\phi,\psi) &= (\sin\phi\sin 2\psi)S_2/2 \,.
\end{aligned} \tag{11}$$

3. COUNTING STATISTICAL ERRORS

An estimate of the errors associated with a measurement is nearly as important as the measurement itself. In determining interplanar spacings by x-ray diffraction, intensities at different points along a diffraction peak are measured to determine the peak position, 2θ. The interplanar spacing may

then be determined from Bragg's law. The intensity measurements are subject to statistical counting error. James and Cohen (1977) give formulae for determining the error in 2θ from the intensity measurements. Estimates of the errors in 2θ can also be determined from nonlinear least-squares fits of peaks to analytical functions.

The variance in e is computed from the variance in 2θ by (Rudnik and Cohen 1986):

$$\mathrm{var}(e) = \left(\frac{1}{do}\right)^2 \left(\frac{\pi}{180}\right)^2 \left(\frac{\lambda \cos\theta}{2\sin 2\theta}\right)^2 \frac{\mathrm{var}(2\theta)}{2} , \qquad (12)$$

where var(2θ) is given by the peak location method. The variance in the strains ε_j may be calculated from the variance in each of the measured strains

$$\mathrm{var}(\varepsilon_j) = \sum_{i=1}^{n} \left(\frac{\delta \varepsilon}{\delta e}\right)^2 \mathrm{var}(e_i) . \qquad (13)$$

The variance in d_o is not considered here but may also be included (Rudnik and Cohen 1986). The errors in the measured strains can be propagated through Equation 9 by using Equation 12 to determine the variance in each of the strains ε_j

$$\mathrm{var}(\varepsilon_j) = \sum_{i=1}^{n} \left(\sum_{j=1}^{6} B^{-1}_{kj} \frac{f_j(\phi_i, U_i)}{\mathrm{var}(e_i)} \right)^2 \mathrm{var}(e_i) . \qquad (14)$$

The variance in each strain value may be evaluated from Equation 13 and used to propagate the error to the stresses using Equations 10 and 12. The errors in the measured stresses may then be estimated from the standard deviations given by the square roots of the variances

$$\mathrm{var}(\sigma_i) = \left(\frac{1}{S_2/2} - \frac{S_1}{S_2/2(S_2/2 + 3S_1)}\right)^2 \mathrm{var}(e_i) + \left(\frac{S_1}{S_2/2(S_2/2 + 3S_1)}\right)^2 [\mathrm{var}(\varepsilon_j) + \mathrm{var}(\varepsilon_k)] \qquad (15a)$$

$$i,j,k = 1,2,3$$

$$\mathrm{var}(\sigma_m) = \left(\frac{1}{S_2/2}\right)^2 \mathrm{var}(\varepsilon_m) \qquad m = 4,5,6\ . \qquad (15b)$$

The counting statistical errors for the Dölle-Hauk method and the generalized least-squares method are compared in Table 1. The diffraction data is taken from sample C3 in Dölle and Cohen (1980). The sample is a normalized plain carbon steel ground along the P_1 direction. The results for the Dölle-Hauk method were calculated using the same program that was used for the calculations in Rudnik and Cohen (1986). The value of d_o was assumed to be known exactly. The standard deviations of the peak posititon, 2θ, were all of the order of 0.012°. These results show that the propagation of error through a generalized least-squares method results in improved counting statistical errors over the Dölle-Hauk method. In the generalized least-squares method each strain measurement e_i contributes to the determination of each strain ε_j to which it is not orthogonal in Equation 2. This is a more efficient use of the available data than the Dölle-Hauk method and results in the improved counting statistical errors.

The counting statistical error in Equation 15 depends only on the errors in e_i and not on the actual values. The tensor of

counting statistical errors will thus be independent of the stress tensor and depends only upon the accuracies to which the interplanar spacings are measured.

It is possible to optimize ϕ_i and ψ_i to minimize the counting statistical errors so that the measurement time to achieve a given error may be minimized. Another consideration, however, is that it is still highly desirable to have a number of ψ-tilts along a constant value of ϕ so that $d_{\phi\psi}$ versus $\sin^2\psi$ plots may be made. These plots provide a valuable visual check that the strains in the sample follow the theory and that the sample was properly aligned during the diffraction measurements (Noyan and Cohen, 1987).

Table 2 illustrates a comparison between use of the "traditional" set of ϕ angles 0°, 45°, and 90° and using the set of 0°, 60°, and 120°. The data is a computer simulation for a steel sample with Cr Kα radiation. Each strain was assumed to have an error of 0.0001. While the normal stresses have the same errors, the errors in the shear stresses are reduced by using ϕ equal to 0°, 60°, and 120°. Thus a greater precision may be obtained in the shear stresses by simply using 0°, 60°, and 120° for ϕ instead of 0°, 45°, and 90°.

4. ERRORS DUE TO GRADIENTS

Noyan (1983) and Noyan and Cohen (1984) have examined the effect of gradients in the stresses on the measurement of

stresses by x-ray diffraction. Since the stresses normal to the surface must be zero at the surface, these stresses must exist as gradients in the sample. The stresses measured by x-ray diffraction are averages measured over the penetration depth of the x-ray beam. In making the measurements, however, the sample must be tilted at different angles to the x-ray beam which gives a different sampling depth for each tilt. Thus the stresses form a different average for each tilt of the sample. Stress gradients, therefore, lead to curvature (but not ψ-splitting) in d versuss $\sin^2\psi$ plots and errors in the measured values of the stresses.

The average stress sampled by an x-ray beam is given by

$$\langle\sigma_{ij}\rangle = \frac{\int_0^\infty \sigma_{ij}(z)\ \exp(-z/\tau)\ dz}{\int_0^\infty \sigma_{ij}(z)\ dz} \quad , \tag{16}$$

where z is the depth into the sample and τ is given by:

$$\tau = \frac{\sin^2\theta - \sin^2\psi}{2\mu\ \sin\theta\ \cos\psi} \quad , \tag{17}$$

for ψ-tilts around the θ-axis (ψ-goniometry) and by:

$$\tau = \frac{\sin\theta\ \cos\psi}{2\mu} \quad , \tag{18}$$

for ψ-tilts around an axis parallel to the plane of the diffractometer (Ω-goniometry).

If we assume, for instance, stress gradients of the form

$$\sigma_{ij}(z) = \sigma_{ij}(0) + a_{ij}z^{n_{ij}} \quad , \tag{19}$$

the average stress becomes

$$\langle\sigma_{ij}\rangle = \sigma_{ij}(0) + K_{ij}\tau^{n_{ij}} \quad , \tag{20}$$

where K_{ij} is a constant. This equation shows that the average stress sampled by the x-ray beam is a function of τ which is a function of the angle Ψ.

When stress gradients are present, as given for example by Equation 19, instead of constant stresses as assumed by the theory, the trigonometric dependence will not be as simple as given in the above equations for $f_j(\phi,\Psi)$ or $g_j(\phi,\Psi)$. There will be a systematic deviation from the theoretical dependence on ϕ and Ψ due to τ, which is a function of Ψ. The averaged stress is further dependent on the unknown gradient. This systematic deviation will cause some error in the measured stress values when Equation 2 is forced to fit the data by any procedure.

To determine the effect and magnitude of these gradient errors and to determine methods to minimize them, computer simulations of stress measurements on samples containing stress gradients were performed similar to those in Noyan (1983) and Noyan and Cohen (1984).

In the computer simulations the sample was assumed to be steel and the measurements done with Cr Kα radiation for the 211 diffraction peak at 156° 2θ for several different stress gradients. The stresses in the plane of the sample surface σ_{11} and σ_{22} were assumed to be uniform. Gradients of the form of Equation 19 were used to calculate an average stress sampled by the x-rays for each Ψ-tilt. Equation 18 for Ω-goniometry was used to determine the value of τ at each Ψ-tilt. A linear absorbtion coefficient of $\mu = 0.09\ \mu m^{-1}$ was used. The measured strain values, e_i, were calculated and these were used to

calculate the measured stresses by the generalized least-squares procedure. Different Ψ-ranges were tested with ϕ equal to 0°, 60°, and 120° in all cases.

Four groups of stress tensors with different gradients were examined to determine the effects of gradients in the different components of the stress tensors. The constants, K_{ij}, were selected to give a value of stress σ_{33} of about 100 MPa for a Ψ-range of 0° to 60° except for the second group of stress tensors for which σ_{33} was zero.

(a) Group I

In group I tensors of the form

$$\sigma = \begin{bmatrix} -400 & 0 & 0 \\ 0 & -400 & 0 \\ 0 & 0 & K\tau^n \end{bmatrix}$$

were examined for n equal to 1, 2, and 3. Table 3 shows the results of the computer simulation with different Ψ-ranges for the measurement while Figure 2 shows the error in the stress σ_{11} as a function of the measured stress σ_{33} for different values of n for the Ψ-range 0-60°. This data shows that the measured value of stress σ_{11} can be greatly affected by a gradient in σ_{33}, especially for low Ψ-ranges. This table also shows that this error can be minimized by using high Ψ-ranges.

(b) Group II

Group II tensors were of the form

$$\sigma = \begin{bmatrix} -400 + K_T{}^n & 0 & 0 \\ 0 & -400 + K_T{}^n & 0 \\ 0 & 0 & 0 \end{bmatrix}.$$

Here the the gradient was in the stresses σ_{11} and σ_{22} and the stress σ_{33} was absent. Again (see Table 4) the high Ψ-range gives the least error in the normal stresses while the low Ψ-range gives the greatest error. The nonzero values of σ_{33} are due to the forced fitting of Equation 2 to the data.

(c) Group III

Combined gradients with tensors of the form

$$\sigma = \begin{bmatrix} -400 + K_{11}T^{n_{11}} & 0 & 0 \\ 0 & -400 + K_{11}T^{n_{11}} & 0 \\ 0 & 0 & K_{33}T^{n_{33}} \end{bmatrix}$$

were examined in group III. Both positive and negative K_{11} were used since values of K_{11} and K_{33} with the same sign have the opposite effect on the curvature in a d versus $\sin^2\Psi$ plot (Cohen et al. 1980). Table 5 shows the results from the group III tensors. When K_{11} and K_{33} have the same sign the error in σ_{11} nearly cancels out depending on the Ψ-range. The low Ψ-range again gives large errors. When K_{11} and K_{33} are of opposite sign

and produce the same curvature in d versus $\sin^2\psi$, the high ψ-range again gives the smallest error in σ_{11}.

(d) Group IV

To test the effect of combined gradients in σ_{33} and σ_{13} group IV tensors were of the form

$$\sigma = \begin{bmatrix} -400 & 0 & K_{33}T^2 \\ 0 & -400 & 0 \\ K_{33}T^2 & 0 & K_{33}T^2 \end{bmatrix} .$$

The results of these tests are shown in Table 6. Once again, the smallest error in the normal stresses is with the high ψ-range. The magnitude of σ_{13} decreases with increasing ψ-range. This is to be expected as the penetration depth of the x-rays decreases with ψ and the high ψ-ranges sample less of the gradient in σ_{13}. Noyan and Cohen (1984) found that the Dölle-Hauk method gave very sporadic results for σ_{13} depending on the ψ-range, sometimes giving the wrong sign. The generalized least-squares method is much more consistent with respect to these shear stresses and will give much more reasonable values for them independent of the ψ-range.

5. CONCLUSIONS

1) A generalized least-squares method of analyzing diffraction data to determine triaxial stress states was presented along with equations to estimate the statistical counting error associated with the measurements. The calculations for a typical triaxial stress measurement such as the one in Table 1 take only a few seconds on a personal computer. Computation time is therefore insignificant in using this analysis method and it is well suited for use in an automated stress measurement system.

2) The d versus $\sin^2\psi$ plots are a valuable visual check on the data and should be used and checked against the results for reasonableness.

3) The use of ϕ equal to 0°, 60°, and 120° will give lower counting statistical error than the traditional values of 0°, 45°, and 90° for the shear stresses.

4) High ψ-ranges minimize the errors in the normal stresses due to stress gradients in the sample. The shear stresses σ_{13} and σ_{23} are adequately measured with any ψ-range, lower ψ-ranges sampling more of their gradient. The method will not give the wrong sign for these stresses as can the Dölle-Hauk method.

5) The generalized least-squares method gives lower statistical counting errors than the Dölle-Hauk method, and smaller errors due to the presence of stress gradients in the sample.

ACKNOWLEDGEMENTS

This research was supported by the Office of Naval Research under contract No. N00014-80-C-116.

REFERENCES

Cohen, J.B., Dölle, H., and James, M.R. (1980). National Bureau of Standards Special Publication 567, 453-477.

Dölle, H., and Hauk, V. (1976). Härterei-Tech. Mitt. 31 [3], 165-169.

Dölle, H. (1979). J. Appl. Cryst. 12, 489-501.

Dölle, H. and Cohen, J.B., (1980). Metall. Trans. A 11, 159-164.

Ho, J.W., Noyan, I.C., Cohen, J.B., Khanna, V.D., and Eliezer, Z. (1983). Wear 84, 183-202.

Imura, T., Weissmann, S., and Slade, J.J., Jr (1962). Acta Crystallogr. 15, 786-793.

James, M.R., and Cohen, J.B. (1977). Adv. X-ray Anal. 20, 291-307.

Marion, R.H., and Cohen, J.B. (1977). Adv. X-ray Anal. 20, 355-367.

Noyan, I.C. (1983). Metall. Trans. A 14, 249-258.

Noyan, I.C. and Cohen, J.B. (1984). Adv. X-ray Anal. 27, 129-149.

Noyan, I.C. (1985). Adv. X-ray Anal. 28, 281-288.

Noyan, I.C., and Cohen, J.B. (1987). 'Residual Stress Determination by Diffraction - Measurement and Interpretation' (Springer-Verlag: New York).

Nye, J.F. (1976) 'Physical Properties of Crystals' (Clarendon: Oxford).

Perry, K., Noyan, I.C., Rudnik, P.J., and Cohen, J.B. (1984). Adv. X-ray Anal. 27, 159-170.

Rudnik, P. and Cohen, J.B. (1986), Adv. X-ray Anal. 29, 79-88.

FIGURE CAPTIONS

FIGURE 1. The coordinate system.

FIGURE 2. Errors due to a gradient in σ_{33}

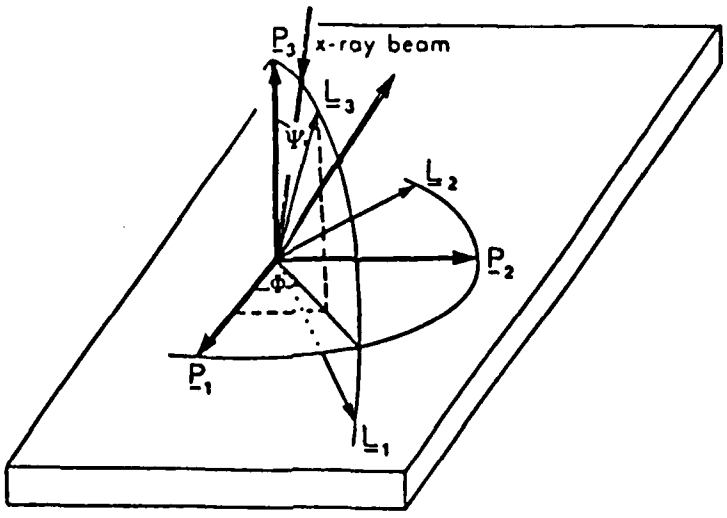

FIGURE 1. R. A. Winholtz and J. B. Cohen

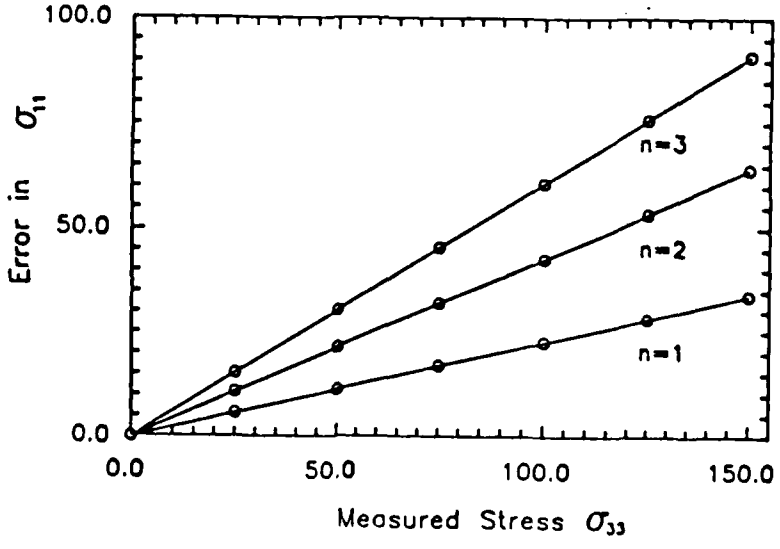

FIGURE 2. R. A. Winholtz and J. B. Cohen

Table 1.

A comparison of the counting statistical errors in the strain and stress (MPa) tensors for the Dölle-Hauk method and a generalized least-squares method*.

$$\varepsilon = \begin{bmatrix} 1.649 & -0.139 & -0.226 \\ -0.139 & 1.721 & 0.013 \\ -0.226 & 0.013 & -1.001 \end{bmatrix} \times 10^{-3} \pm \begin{bmatrix} 0.088 & 0.087 & 0.026 \\ 0.087 & 0.080 & 0.021 \\ 0.026 & 0.021 & 0.064 \end{bmatrix} \times 10^{-3}$$

$$\sigma = \begin{bmatrix} 539.74 & -24.03 & -39.15 \\ -24.03 & 552.16 & 2.30 \\ -39.15 & 2.30 & 80.41 \end{bmatrix} \pm \begin{bmatrix} 27.08 & 15.05 & 4.58 \\ 15.05 & 25.30 & 3.56 \\ 4.58 & 3.56 & 21.97 \end{bmatrix}$$

(a) Dölle-Hauk

$$\varepsilon = \begin{bmatrix} 1.515 & -0.045 & -0.234 \\ -0.045 & 1.888 & 0.029 \\ -0.234 & 0.029 & -0.936 \end{bmatrix} \times 10^{-3} \pm \begin{bmatrix} 0.036 & 0.043 & 0.010 \\ 0.043 & 0.031 & 0.009 \\ 0.010 & 0.009 & 0.010 \end{bmatrix} \times 10^{-3}$$

$$\sigma = \begin{bmatrix} 527.04 & -7.90 & -40.48 \\ -7.90 & 591.73 & 4.99 \\ -40.48 & 4.99 & 49.87 \end{bmatrix} \pm \begin{bmatrix} 10.73 & 7.39 & 1.72 \\ 7.39 & 9.59 & 1.53 \\ 1.72 & 1.53 & 5.82 \end{bmatrix}$$

(b) Generalized Least-Squares

*The data is from a ground steel sample. Analysis from the Dölle-Hauk method is given in (a) and from a generalized least-squares method in (b).

Table 2.

A comparison of the counting statistical errors in the strain and stress (MPa) tensors for the use of (a) ϕ = 0°, 45°, and (b) 90° and ϕ = 0°, 60°, and 120° *.

$$\varepsilon = \begin{bmatrix} 1.308 & 0.000 & 0.000 \\ 0.000 & 1.308 & 0.000 \\ 0.000 & 0.000 & 1.000 \end{bmatrix} \times 10^{-3} \pm \begin{bmatrix} 0.117 & 0.117 & 0.031 \\ 0.117 & 0.117 & 0.031 \\ 0.031 & 0.031 & 0.039 \end{bmatrix} \times 10^{-3}$$

$$\sigma = \begin{bmatrix} -400.00 & 0.00 & 0.00 \\ 0.00 & -400.00 & 0.00 \\ 0.00 & 0.00 & 0.00 \end{bmatrix} \pm \begin{bmatrix} 35.43 & 20.24 & 5.44 \\ 20.24 & 35.43 & 5.44 \\ 5.44 & 5.44 & 20.91 \end{bmatrix}$$

(a) ϕ = 0°, 45°, and 90°

$$\varepsilon = \begin{bmatrix} 1.308 & 0.000 & 0.000 \\ 0.000 & 1.308 & 0.000 \\ 0.000 & 0.000 & 1.000 \end{bmatrix} \times 10^{-3} \pm \begin{bmatrix} 0.117 & 0.078 & 0.030 \\ 0.078 & 0.117 & 0.030 \\ 0.117 & 0.030 & 0.039 \end{bmatrix} \times 10^{-3}$$

$$\sigma = \begin{bmatrix} -400.00 & 0.00 & 0.00 \\ 0.00 & -400.00 & 0.00 \\ 0.00 & 0.00 & 0.00 \end{bmatrix} \pm \begin{bmatrix} 35.43 & 13.49 & 5.13 \\ 13.49 & 35.43 & 5.13 \\ 5.13 & 5.13 & 20.91 \end{bmatrix}$$

(b) ϕ = 0°, 60°, and 120°

*The results are a computer simulation for a steel sample measured with Cr Kα radiation at 2θ = 156°. Each strain was assumed to have an error of 0.0001.

Table 3.

Computer Simulation Results for Group I Stress Tensors.

n_{33}	K_{33}	Ψ-Range (Degrees)	σ_{11} (MPa)	σ_{33} (MPa)	$\lvert\sigma_{11} - \sigma_{11}\rvert$ (MPa)
1	22.6764	0.00 - 60.00	-422.6	100.0	22.6
1	22.6764	0.00 - 33.21	-476.0	79.4	76.0
1	22.6764	39.23 - 60.00	-407.5	88.3	7.5
2	5.0243	0.00 - 60.00	-442.8	100.0	42.8
2	5.0243	0.00 - 33.21	-564.2	52.6	164.2
2	5.0243	39.23 - 60.00	-411.5	76.5	11.5
3	1.0920	0.00 - 60.00	-460.7	100.0	60.7
3	1.0920	0.00 - 33.21	-661.6	20.8	261.6
3	1.0920	39.23 - 60.00	-413.2	65.3	13.2

Table 4.

Computer Simulation Results for Group II Tensors

n_{11}	K_{11}	Φ-Range (Degrees)	σ_{11} (MPa)	σ_{33} (MPa)	Error in σ_{11} (MPa)
1	10.00	0.00 - 60.00	-366.2	-5.7	33.8
1	10.00	0.00 - 33.21	-337.8	5.2	62.2
1	10.00	39.23 - 60.00	-374.4	0.7	25.6
2	2.50	0.00 - 60.00	-367.7	-10.7	32.3
2	2.50	0.00 - 33.21	-307.5	12.8	92.5
2	2.50	39.23 - 60.00	-383.2	0.9	16.8
3	0.55	0.00 - 60.00	-369.8	-13.9	30.2
3	0.55	0.00 - 33.21	-282.2	20.8	127.8
3	0.55	39.23 - 60.00	-389.9	0.7	10.1

Table 5.

Computer Simulation Results for Group III Tensors

n_{11}	K_{11}	n_{33}	K_{33}	Ψ-Range (Degrees)	σ_{11} (MPa)	σ_{33} (MPa)	$\lvert\sigma_{11} - \sigma_{11}\rvert$ (MPa)
1	10.0	2	5.0	0.00 - 60.00	-408.7	93.8	8.7
1	10.0	2	5.0	0.00 - 33.21	-501.3	57.6	101.3
1	10.0	2	5.0	39.23 - 60.00	-385.9	76.9	14.1
2	2.0	2	5.0	0.00 - 60.00	-416.7	91.0	16.7
2	2.0	2	5.0	0.00 - 33.21	-489.4	62.6	89.4
2	2.0	2	5.0	39.23 - 60.00	-398.0	76.9	2.0
1	-10.0	2	5.0	0.00 - 60.00	-476.4	105.2	76.4
1	-10.0	2	5.0	0.00 - 33.21	-625.6	47.1	225.6
1	-10.0	2	5.0	39.23 - 60.00	-437.0	75.4	37.0
2	-2.0	2	5.0	0.00 - 60.00	-468.4	105.1	68.4
2	-2.0	2	5.0	0.00 - 33.21	-637.4	42.1	237.4
2	-2.0	2	5.0	39.23 - 60.00	-424.9	75.4	24.9

Table 6.

Computer Simulation Results for Group IV Tensors

n_{33}	K_{33}	Ψ-Range (Degrees)	σ_{11} (MPa)	σ_{33} (MPa)	σ_{13} (MPa)	$\lvert\sigma_{11} - \sigma_{11}\rvert$ (MPa)
2	5.0	0.00 - 60.00	-442.6	99.5	76.6	42.6
2	5.0	0.00 - 33.21	-563.4	52.3	111.2	163.4
2	5.0	39.23 - 60.00	-411.5	76.1	59.2	11.5
2	5.0	0.00 - 26.57	--	--	121.3	--
2	5.0	33.21 - 45.00	--	--	80.6	--
2	5.0	50.77 - 60.00	--	--	44.2	--

Security Classification

AD-A183 851

DOCUMENT CONTROL DATA - R & D

Security classification of title, body of abstract and indexing annotation must be entered when the overall report is classified)

1. ORIGINATING ACTIVITY (Corporate author)	2a. REPORT SECURITY CLASSIFICATION
J. B. Cohen Northwestern University The Technological Institute, Evanston, IL 60208	2b. GROUP

3. REPORT TITLE

A GENERALIZED LEAST-SQUARES DETERMINATION OF TRIAXIAL STRESS STATES BY X-RAY DIFFRACTION AND THE ASSOCIATED ERRORS

4. DESCRIPTIVE NOTES (Type of report and inclusive dates)

TECHNICAL REPORT #25

5. AUTHOR(S) (First name, middle initial, last name)

R. A. Winholtz, and J. B. Cohen

6. REPORT DATE	7a. TOTAL NO. OF PAGES	7b. NO. OF REFS
JULY 1987	24	

8a. CONTRACT OR GRANT NO.	9a. ORIGINATOR'S REPORT NUMBER(S)
N00014-80-c-116	#25
b. PROJECT NO.	
c.	9b. OTHER REPORT NO(S) (Any other numbers that may be assigned this report)
d.	

10. DISTRIBUTION STATEMENT

Distribution of document is unlimited

11. SUPPLEMENTARY NOTES	12. SPONSORING MILITARY ACTIVITY
	Metallurgy Branch Office of Naval Research

13. ABSTRACT

The determination of residual stresses via x-ray diffraction is briefly reviewed, with particular emphasis on the triaxial stress state. A new method is proposed for determining the general stress tensor, which considerably reduces the variances of the stresses due to counting statistics and gradients. The procedure involves a generalized least-squares solution of strains measured at various tilts of the x-ray beam to the sample, and a set of tilts not heretofore used is recommended to minimize these errors.

DD FORM 1 NOV 65 1473 (PAGE 1)

S/N 0101-807-6801

Security Classification

END

9-87

DTIC